

NONCOMMUTATIVE MODEL SELECTION FOR DATA CLUSTERING AND DIMENSION REDUCTION USING RELATIVE VON NEUMANN ENTROPY

ARACELI GUZMÁN-TRISTÁN AND ANTONIO RIESER*

ABSTRACT. We propose a pair of completely data-driven algorithms for unsupervised classification and dimension reduction, and we empirically study their performance on a number of data sets, both simulated data in three-dimensions and images from the COIL-20 data set. The algorithms take as input a set of points sampled from a uniform distribution supported on a metric space, the latter embedded in an ambient metric space, and they output a clustering or reduction of dimension of the data. They work by constructing a natural family of graphs from the data and selecting the graph which maximizes the relative von Neumann entropy of certain normalized heat operators constructed from the graphs. Once the appropriate graph is selected, the eigenvectors of the graph Laplacian may be used to reduce the dimension of the data, and clusters in the data may be identified with the kernel of the associated graph Laplacian. Notably, these algorithms do not require information about the size of a neighborhood or the desired number of clusters as input, in contrast to popular algorithms such as k -means, and even more modern spectral methods such as Laplacian eigenmaps, among others.

In our computational experiments, our clustering algorithm outperforms k -means clustering on data sets with non-trivial geometry and topology, in particular data whose clusters are not concentrated around a specific point, and our dimension reduction algorithm is shown to work well in several simple examples.

1. INTRODUCTION

Unsupervised clustering and dimension reduction are two of the most important and difficult problems in modern data analysis, as well as one of the most ubiquitous, appearing in nearly every area of data science, including image processing, bioinformatics, and natural language processing, among others. Most popular unsupervised clustering algorithms, including classical methods such as k -means ([11], Section 14.3.6), in addition to many more recently proposed techniques [3, 16, 5, 1, 9, 18, 20, 7, 2, 17], depend on additional data which must be chosen by the user in order to run, and which keeps these methods from being completely data-driven. In this paper, we propose

*Corresponding author.

Araceli Guzmán-Tristán was supported by the CONAHCYT program "Estancias Posdoctorales por México para la Formación y Consolidación de las y los Investigadores por México". Antonio Rieser was supported by the US National Science Foundation under grants No. DMS-1929284 and DMS-1928930, the first while in residence at the Institute for Computational and Experimental Research in Mathematics in Providence, RI, during the "Math + Neuroscience: Strengthening the Interplay Between Theory and Mathematics" program, and the second while in residence at the Simons-Laufer Mathematical Sciences Research Institute in the spring of 2024 and in a program supported by the Mathematical Sciences Research Institute in the summer of 2022, held in partnership with the the Universidad Nacional Autónoma de México. Antonio Rieser was also supported by the CONAHCYT Investigadoras y Investigadores por México Project #1076 and by the grant N62909-19-1-2134 from the US Office of Naval Research Global and the Southern Office of Aerospace Research and Development of the US Air Force Office of Scientific Research.

new spectral clustering and dimension reduction algorithms in which their free parameters may be chosen by considering the noncommutative information-theoretic aspects of these problems.

Following [13], we interpret the clustering problem to be the problem of assigning each point in a data set S to the closest connected component of the support X of a probability distribution μ from which the data was sampled (perhaps with additional noise). Our algorithm works by constructing a family of weighted graphs G_r for each $r > 0$, where the vertices of G_r are the data points and the points are connected if they are within a distance r of one another, with weights given by the ambient distance between two points. If one considers the heat semigroup on each graph as a heat flow on the vertices, then the resulting steady state of the flow on G_r is constant on the connected components of each G_r . We also adopt the model-selection heuristic used in [13]: that the optimal graph in the family of graphs should be the one for which the diffusion process generated by the graph Laplacian is relatively local initially, but relatively global at the steady state. We measure this by calculating the relative von Neumann entropy between the (normalized) heat operator at $t = 1$ and the (normalized) heat operator at a second time $t' \gg 1$, the latter of which we interpret as an estimate of limit of the relative von Neumann entropy between the two operators as $t' \rightarrow \infty$. Choosing the graph where this relative von Neumann entropy is maximal then produces a graph which is balanced between vertices being very connected at short distances but not particularly connected at long distances. Once the graph is chosen, the number of connected components of the graph is the dimension of the kernel of its Laplacian matrix, and each point can then be algorithmically assigned to its connected component as in [13] by analyzing the null space of the graph Laplacian. Alternately, one may use the chosen graph to reduce the dimension of the data set by using the eigenvectors of the graph Laplacian to construct a map from the data set S to \mathbb{R}^k for some small integer k as is typically done in Laplacian Eigenmaps [3] and Diffusion Maps [7]. In our experiments, the algorithm improved on the average relative entropy method in [13] when applied to graphs whose edges were defined using Euclidean balls around each point, and outperformed k -means on several examples using simulated data as well as the unprocessed images from the COIL-20 image database.

1.1. Contributions and Related Work. A difficult problem inherent to many spectral approaches to dimension reduction and clustering, including local linear embedding [14], Laplacian eigenmaps [3], Hessian eigenmaps [9], isomap [18], local tangent space alignment [20], diffusion maps [7], and vector diffusion maps [17], is how to systematically choose the free parameter necessary to run the algorithms. Indeed, most current practitioners simply choose these parameters by hand on an ad hoc basis after some trial and error. To the best of our knowledge, there are two earlier works which have proposed methods for resolving this issue. In [13], the second author of the present article proposed two new methods for automatic clustering, each of which consisted of a heuristic for selecting a graph from a family of graphs by examining the action of the heat semigroup on a basis for the functions from the data set to \mathbb{R} , and which then analyzed the kernel of the relevant graph Laplacian to identify the connected components of the chosen graph. In [15], a heuristic based on the semigroup property of the operators constructed in diffusion maps was developed for selecting the free parameter in that method. We remark that these algorithms are not interchangeable. The semigroup technique from [15] is not expected to work in the setting of the current article (or that in [13]), because the free parameter $r > 0$ in [13] and the present article is no longer a priori coupled to the semigroup parameter. Conversely, we do not expect that either the Average Local Volume Method or the Average Relative Entropy Method from [13] can be made to work with diffusion maps, since they both depend on the fact the the graphs in question are

disconnected for sufficiently small radii, and all the graphs in diffusion maps are connected (and, indeed, they are even complete graphs on the vertices).

In this article, we make two main contributions to the literature on spectral clustering and dimension reduction. First, we introduce a new spectral method which uses the ambient distances between points (up to some distance r) for the weights in our graphs, instead of the similarity kernels which are more typically used, and we demonstrate empirically that the spectral properties of the Laplacians and heat semigroups of such graphs may also be used for clustering and dimension reduction. This simplifies the construction of the graphs relative to the standard constructions, and it also clarifies that graph approximations of a metric space can be taken to be geometric models of the underlying space, and, furthermore, that the diffusion processes analyzed in the subsequent clustering and dimension reduction techniques may be built on top of the geometry encoded in the edge weights of the graphs, instead of guessed a priori. Second, and most importantly, we propose a method for selecting a geometric graph model of a metric space from a one-parameter family of such models. We do so by maximizing the relative von Neumann entropy between an operator in the heat semigroup for a graphs $\{G_r\}_{r>0}$ at some finite time (in this case $t = 1$) and an approximation of the operator representing the steady state of the diffusion process. This builds and improves on the methods introduced in [13], and it introduces genuinely noncommutative tools into the model selection process for data clustering and dimension reduction. We give a number of experimental demonstrations that the choices of edge weights and model selection techniques introduced here produce good results for the data clustering and dimension reduction problems, using both simulated and real data sets.

2. GRAPH MODELS AND MODEL SELECTION

2.1. Graphs, Laplacians, and Heat Semigroups. As in [13], we assume that our data set S has been sampled from a disconnected metric measure space (X, d_X, μ) , possibly with noise, and we wish to assign each point $x \in S$ to the closest connected component $X_i \subset X$. The number of connected components of X is a topological invariant, and so one of our aims will be to incorporate topological techniques into the solution to this problem, following the general ideas in [13].

We begin with some basic preliminaries on graph Laplacians and the semigroups they generate. For any finite, weighted, undirected graph $G = (V, E, w)$, where G contains no loops, i.e. $(x, x) \notin E$ for all $x \in V$, and $w : E \rightarrow (0, \infty)$ is a function which assigns a positive weight to every edge, we define the *Laplacian matrix of the graph G* , L_G , by

$$(1) \quad (L_G)_{(i,j)} = \begin{cases} -w(x_i, x_j) & \text{if } (x_i, x_j) \in E, \\ 0 & \text{if } (x_i, x_j) \notin E \text{ and } i \neq j \\ \sum_{(x_i, x_k) \in E} w(x_i, x_k) & \text{if } i = j. \end{cases}$$

We also define the corresponding heat operators e^{-tL_G} for $t \in [0, \infty)$. Note that $e^{-tL_G}e^{-sL_G} = e^{-(t+s)L_G}$, so $\{e^{-tL_G}\}_{t \in [0, \infty)}$ forms a semigroup under matrix multiplication, which we call the *heat semigroup of G* .

To find the connected components of a graph G , we will appeal to the following well-known facts (see, for instance, Lemma 1.7(iv) in [6]):

Theorem 1. *The number of connected components of a graph G is equal to the dimension of the kernel of L_G .*

Theorem 2. *Each eigenfunction $f \in \ker L_G$ is constant on each connected component of G .*

Note that the operators L_G and e^{-tL_G} act on the space of functions $\{f : V_G \rightarrow \mathbb{R}\}$. The above theorems imply that the clustering problem can be solved if we can find a basis for $\ker L_G$ such that each basis function is non-zero and constant on one of the clusters and zero otherwise.

For the dimension reduction problem, we wish to embed the data set S in to \mathbb{R}^k in a way which preserves the local structure of S as much as possible. The spectral methods for doing so all are loosely based on the following classical theorem by Bérard, Besson, and Gallot [4] on embeddings of a Riemannian manifold into ℓ^2 . We begin with a preliminary definition.

Definition 1. Let M be an n -dimensional closed manifold and let $a := \{\phi_j\}_{j \geq 0}$ be an orthonormal basis of the Laplacian of M . Define the family of maps $\psi_t^a : M \rightarrow \ell^2$, $t > 0$ by

$$\psi_t^a(x) := \sqrt{2(4\pi)^{n/4}t^{(n+2)/4}} \left\{ e^{-\lambda_j t/2} \phi_j^a(x) \right\}_{j \geq 1}$$

Theorem 3. Let (M, g) be a closed Riemannian manifold and let $a = \{\phi_j^a\}_{j \geq 0}$ be an orthonormal basis of its Laplacian. Let g_E denote the usual Euclidean scalar product on ℓ^2 . then

- (1) For all positive t , the map ψ_t^a is an embedding of M into ℓ^2 .
- (2) the pull-back metric $(\psi_t^a)^* g_{can}$ is asymptotic to the metric g of M when $t \rightarrow 0_+$.

For the purposes of dimension reduction, this theorem implies that, for some fixed but sufficiently small t , the map $S \rightarrow \mathbb{R}^k$ given by

$$x \mapsto \{\phi_t^a(x)\}_{1 \leq j \leq k}$$

may be seen as an approximation of the map ψ_t^a , up to a multiplicative constant which depends on the intrinsic dimension of the manifold, and it therefore approximately preserves the local geometry encoded in the Riemannian metric (again, up to some constant coefficients).

2.2. The Clustering and Dimension Reduction Problems. Our approach to both the data clustering and dimension reduction problems center around choosing a weighted graph which best estimates the intrinsic geometry of the data from a family of possible graphs.

We now define the family of weighted graphs we will consider. Let $S \subset (X, d_X)$ be a finite subset of a metric space (X, d_X) which itself has been embedded in another metric space (Z, d_Z) . We further suppose that, for every $x \in X$,

$$\lim_{X \ni x' \rightarrow x} \frac{d_Z(x, x')}{d_X(x, x')} = 1.$$

This guarantees that $d_Z(x, x')$ and $d_X(x, x')$ are close for $d_X(x, x')$ (or $d_Z(x, x')$) sufficiently small. For each real number $r > 0$, let $G_r = (V_r, E_r, w)$ be a weighted graph, where V_r , E_r , and $w : E_r \rightarrow \mathbb{R}$ are defined by

$$\begin{aligned} V_r &= S, \\ E_r &= \{(x, x') \in V_r \times V_r \mid d(x, x') \leq r\} \\ w(x, x') &= d_Z(x, x') \end{aligned}$$

That is, the vertices of G_r are the points in the data set, and two vertices are connected by an edge if they lie in a ball of radius r centered at one of them, and the weight of each edge is the ambient distance in Z between the vertices. Note that these weights are quite different from those used in in Laplacian Eigenmaps [3] or Diffusion Maps [7], where the weights use a heat kernel $K_r : \mathbb{R}^n \times \mathbb{R}^n \rightarrow \mathbb{R}$ defined on the ambient space \mathbb{R}^n , which is meant to provide a local estimate of a diffusion kernel on X evaluated at the vertices of each edge. Also the graphs G_r are not fully connected in general, unlike in Laplacian eigenmaps and diffusion maps. No edge is added between

any pair of vertices x, x' with $d_Z(x, x') > r$. In fact, the graphs G_r will be completely disconnected for sufficiently small $r > 0$.

Once we have the graphs G_r , to solve the clustering problem, we must choose a scale $\hat{r} > 0$ so that the connected components of the graph $G_{\hat{r}}$ at this scale best approximate the connected components of X . For the dimension reduction problem, on the other hand, we would like to choose a scale $\hat{r} > 0$ and an embedding $\Phi : S \rightarrow \mathbb{R}^k$, $k < n$, of the form

$$\Phi(x) := (\hat{\phi}_0(x), \hat{\phi}_1(x), \dots, \hat{\phi}_k(x)),$$

where the $\hat{\phi}_i$ are the eigenfunctions of $L_{G_{\hat{r}}}$, so that the local geometry of (X, d_X) restricted to S is as well-preserved as possible in the image of $S \subset \mathbb{R}^k$.

2.3. Relative von Neumann Entropy. Quantum information theory has provided many new tools and insights with which to study linear operators and operator algebras, motivated by the need to provide a solid theoretical foundation for quantum computation and quantum communication. While the computational setting of the present work is unequivocally classical, we are nonetheless confronted with families of noncommutative Hermitian operators, a setting in which many of the constructions of quantum information theory are quite natural. In the algorithms and experiments which follow, we will see that these quantum constructions not only apply in this context, but they also reveal important information about the collection of graphs $\{G_r\}_{r>0}$ and they are essential to our model selection algorithms. In this section, we collect the basic definitions and results from quantum information theory that we will require.

Definition 2. *Let H be a Hilbert space. A positive operator A on H is defined to be an operator such that for any vector $v \in H$, the inner product $\langle v, Av \rangle_H$ is a real, non-negative number. If, in addition, $\langle v, Av \rangle_H > 0$ for all $v \neq 0$, then we say that the operator A is positive definite.*

Remark 1. We recall that any positive operator has non-negative eigenvalues, and any positive definite operator has strictly positive eigenvalues. See [8] for this and other properties of positive operators on Hilbert spaces.

Following physics terminology, we define a density operator as follows.

Definition 3. *A positive operator ρ is called a density operator iff $\text{Tr}(\rho) = 1$.*

We now define the relative von Neumann entropy, also known as the relative quantum entropy.

Definition 4. *Let the support of an operator ρ on a Hilbert space H be the set*

$$\text{supp } \rho := \{v \in H \mid \rho(v) \neq 0\}.$$

Suppose that ρ is a density operator, and let σ be a positive operator. We define the relative von Neumann entropy or relative quantum entropy $H(\rho||\sigma)$ of ρ and σ by

$$H(\rho||\sigma) := \begin{cases} \text{Tr}(\rho \log(\rho) - \rho \log(\sigma)) & \text{if } \text{supp } \rho \subseteq \text{supp } \sigma \\ +\infty & \text{Otherwise.} \end{cases}$$

Although the relative von Neumann entropy is neither symmetric nor satisfies the triangle inequality, it nonetheless provides a useful way to compare positive operators with trace between 0 and 1. In particular, we have

Proposition 1. *[19], Theorem 11.8.2 If ρ is a density operator and $0 \leq \text{Tr}(\sigma) \leq 1$, then $H(\rho||\sigma)$ is non-negative. In addition, under these conditions, $H(\rho||\sigma) = 0$ iff $\sigma = \rho$.*

In some special cases, the relative von Neumann entropy reduces to the relative Shannon entropy of the eigenvalues of the operators, viewed as distributions on a finite space. We will use following case in our algorithms.

Proposition 2. *Let ρ be a density operator on a finite dimensional vector space V . If σ is a positive semi-definite operator such that $\text{supp } \rho \subseteq \text{supp } \sigma$ and ρ and σ are simultaneously diagonalizable, then*

$$H(\rho||\sigma) = \sum_i \lambda_i^\rho \log \lambda_i^\rho - \lambda_i^\rho \log \lambda_i^\sigma,$$

where the λ_i^ρ are the eigenvalues of ρ and the λ_i^σ are the eigenvalues of σ .

Proof. If the matrices ρ and σ are simultaneously diagonalizable, then the expression above is the sum of the eigenvalues of $\rho \log \rho - \rho \log \sigma$, which is equal to the trace. \square

2.4. Selecting the Model. We now describe our model selection procedure for both the clustering and dimension reduction problems, which may be seen as a genuinely noncommutative version of the Average Maximum Relative Entropy Method in [13]. Let S be a collection of n points in a metric space (X, d) , and for each $0 < r < \text{diam}(S)$, let G_r be the graph defined in Section 2.1. Let L_r denote the graph Laplacian of G_r and let $\{e^{-tL_r}\}_{t=0}^\infty$ be the resulting heat semigroup. The heuristic behind our model selection algorithm is that the operators e^{-tL_r} for low values of t reflect the local combinatorial and geometric structure of the graph G_r . That is, for low values of t , given a function $f : V \rightarrow V$ which takes the value 1 at a vertex v and is 0 elsewhere, the function $e^{-tL_r} f$ is supported close to v . On the other hand, when $t \rightarrow \infty$ the heat semigroup converges to a steady state, erasing the local geometry, but giving the connected components of G_r . We wish to choose an $r > 0$ such that the local geometry of G_r reflected in e^{-L_r} (with $t = 1$) is as different as possible from the steady state $\lim_{t \rightarrow \infty} e^{-tL_r}$. We might like to measure this difference by the limit of the relative entropies as $t \rightarrow \infty$, however, since the trace of the heat operators $\text{Tr}(e^{-tL_r})$ may be larger than 1 a priori, we first normalize the operators before calculating the relative entropy. Our experiments confirm that this is a useful metric. Our selected scale \hat{r} will therefore be

$$(2) \quad \hat{r} := \text{argmax} \left(\lim_{t \rightarrow \infty} H \left(\frac{1}{\text{Tr}(e^{-L_r})} e^{-L_r} \middle| \middle| \frac{1}{\text{Tr}(e^{-tL_r})} e^{-tL_r} \right) \right),$$

In practice, it is sufficient to use $t \gg 1$, large enough so that the eigenvalues of e^{-tL_r} are close to either 0 or 1. Once we have computed \hat{r} , we construct a map $\Psi : V \rightarrow \mathbb{R}^{\dim \ker L_{\hat{r}}}$ as in [13] (see also Algorithm 2 below) which sends the vertices in the i -th connected component of $G_{\hat{r}}$ to the standard basis vector $e_i \in \mathbb{R}^{\dim \ker L_{\hat{r}}}$. To identify the clusters, we then take the inverse image of each of the $e_i \in \mathbb{R}^{\dim \ker L_{\hat{r}}}$.

3. THE ALGORITHMS

We present three algorithms below: the clustering algorithm, a modified Gaussian elimination algorithm used in the clustering algorithm to identify the clusters from the kernel of a graph Laplacian, and the dimension reduction algorithm. In both the clustering and dimension reduction algorithms, the input is a finite collection of points S in a metric spaces, and for every $r < \text{Diam}(S)$, we construct the graph G_r using the Euclidean distance between points, and we construct L_r , e^{-L_r} , and $e^{-t^*L_r}$ as in Section 2.1, where $t^* \gg 0$ is sufficiently large that all the eigenvalues of $e^{-t^*L_r}$ are either close to 0 or close to 1. The target scale in both cases is chosen according to Equation (2). In the clustering algorithm, we calculate the kernel of the Laplacian at the target scale, and then use the modified Gaussian elimination algorithm (Algorithm 2) to identify the clusters. In

the dimension reduction algorithm (Algorithm 3 below), once we have identified the target scale, we use the first k eigenvectors, $k < n$ of the Laplacian $L_{\hat{r}}$ to define a map $\Psi : S \rightarrow \mathbb{R}^k$ by $\Psi(x) = (\phi_1(x), \dots, \phi_k(x))$. The dimension k of the dimension reduction is chosen by the user.

Algorithm 1 Clustering Algorithm

- 1: **for** $r < \text{Diam}(S)$ **do**
 - 2: Compute $G_r, L_r, \exp(-L_r)$ and estimate $\lim_{t \rightarrow \infty} \exp(-tL_r)$ by $\exp(-t^*L_r)$ for some t^* large.
 - 3: Compute the relative von Neumann entropy $S_r(\rho||\sigma)$ where $\rho = \frac{1}{\text{tr}(\exp(-L_r))} \exp(-L_r)$ and $\sigma = \frac{1}{\text{tr}(\exp(-1000L_r))} \exp(-1000L_r)$
 - 4: **end for**
 - 5: Define $\hat{r} := \text{argmax}_r S_r$.
 - 6: Compute a basis for the kernel of $L_{\hat{r}}$, i.e. ϕ_i for $i \in 1, \dots, k$.
 - 7: Using Algorithm 2 and the ϕ_i , create the map $\Psi : z_m \rightarrow \Psi(z_m) = (\psi_1(z_m), \psi_2(z_m), \dots, \psi_k(z_m)) \in \mathbb{R}^k$.
 - 8: Compute the distances $d_i(z_m) := \|\Psi(z_m) - e_i\|$ for each point z_m in the sample.
 - 9: Assign the vertex m to the i -th cluster if $d_i(z_m) < d_j(z_m)$ for all $j \neq i$.
-

The modified Gaussian elimination algorithm (Algorithm 2 below) takes a matrix whose rows span the kernel of a graph Laplacian - and so each row is constant on connected components of the graph - and outputs a matrix whose entries are either (very close to) 1 or (very close to) 0, and where each row is supported (up to a small error) on exactly one connected component of the graph. The clusters are then identified as the support of each row. This algorithm was also used in the clustering methods in [13]

Algorithm 2 Modified Gaussian elimination Ψ

- 1: **for** $i = 1$ to k **do**
 - 2: Reorder columns i through n of Ψ so that $|\Psi_{(i,i)}|$ is the maximum of $|\Psi_{(i,j)}|$ in row i .
 - 3: Divide row i by $\Psi_{(i,i)}$
 - 4: Using elementary row operations, make $\Psi_{(k,i)} = 0$ for $k \neq i$.
 - 5: **end for**
 - 6: Redefine $\psi_i := \Psi_{i,*}$, and (abusing notation) using the new ψ_i , redefine the map $\Psi(z_m) := (\psi_1(z_m), \psi_2(z_m), \dots, \psi_k(z_m))$.
-

4. EXPERIMENTAL RESULTS

4.1. Clustering. We now present the results of the numerical experiments we ran to test the data clustering and dimension reduction algorithms, as well as comparisons to k -means clustering. We tested the data clustering algorithm on both synthetic data and the unprocessed COIL-20 image database [12], the latter of which consists of 72 images of each of five objects, where each object is rotated five degrees around a vertical axis between one image and the next. The dimension reduction algorithm was tested on a number of shapes in \mathbb{R}^3 and then reduced to shapes in \mathbb{R}^2 in order to facilitate the visualization of the results.

Algorithm 3 Dimension Reduction Algorithm

-
- 1: **for** $r < \text{Diam}(S)$ **do**
 - 2: Compute $G_r, L_r, \exp(-L_r)$ and estimate $\lim_{t \rightarrow \infty} \exp(-tL_r)$ by $\exp(-t^*L_r)$ for some t^* large.
 - 3: Compute the relative von Neumann entropy $S_r(\rho||\sigma)$ where $\rho = \frac{1}{\text{tr}(\exp(-L_r))} \exp(-L_r)$ and $\sigma = \frac{1}{\text{tr}(\exp(-1000L_r))} \exp(-1000L_r)$
 - 4: **end for**
 - 5: Define $\hat{r} := \text{argmax}_r S_r$.
 - 6: Compute the eigenvalues of $L_{\hat{r}}$ and sort them in ascending order $\lambda_0 = 0 < \lambda_1 < \dots < \lambda_n < 1$.
 - 7: Discard the 0 eigenvalue and take the corresponding eigenvectors $\Psi_1, \Psi_2, \dots, \Psi_n$.
 - 8: Let $k < n$ be the target dimension, then the embedding map from X to \mathbb{R}^k is $\Psi(x) = \begin{pmatrix} \phi_1(x) \\ \phi_2(x) \\ \vdots \\ \phi_k(x) \end{pmatrix}$.
-

4.2. Relative Entropy Clustering Results. Tables 1 and 3 summarize the results (the number β_0 of clusters) produced by the clustering algorithm on data sets of 500 and 1000 points sampled from three interlinked circles embedded in \mathbb{R}^3 with a small amount of Gaussian noise (standard deviation SD). Images of the samples, colored according to the results of the clustering algorithm, are shown in Figures 1-8. The horizontal circle has radius 1 and center $(0, 0, 0)$, and the other have radii 0.5 and 0.4 and centers $(0, -1, 0)$ and $(0, 1, 0)$, respectively. For the clustering algorithm, the graphs G_r were obtained the Euclidean distance between points as the edge weights and the calculation of the relative entropy used $t^* = 1000$. We ran five different trials, where the Gaussian noise had standard deviations of 0.01, 0.02, 0.03, 0.04, and 0.05. For each standard deviation value, we repeated the experiment 150 times. In each trial, the relative von Neumann entropy was computed for 200 values of r .

TABLE 1. Relative von Neumann entropy Method, 500 sample points

$SD \beta_0$	1	2	3	>4
0.01	0	6.667	93.334	0
0.02	0	64.667	35.334	0
0.03	2.667	92	5.334	0
0.04	31.334	68.667	0	0
0.05	77.334	22.667	0	0

TABLE 2. Each row in the table contains the results of the trial for points samples at the corresponding noise level (SD in the table). The number in each cell is the percent of the experiments for that noise level whose output (β_0) was the value at the top of the column.

Comparing these results with those obtained in the model selection by average relative entropy (the ARE method) in [13], we see that this method represents a significant improvement. For example, in the case of 500 points and standard deviation of noise equal to 0.01, the ARE method in [13] returns the correct number of clusters for 64% of the trials, compared with the 93.334% in

TABLE 3. Relative von Neumann entropy Method, 1000 sample points

$SD \beta_0$	1	2	3	>4
0.01	0	0	100	0
0.02	0	0	100	0
0.03	0	1.334	98.667	0
0.04	0	51.334	48.667	0
0.05	0	96.667	3.334	0

TABLE 4. Each row in the table contains the results of the trial for points samples at the corresponding noise level (SD in the table). The number in each cell is the percent of the experiments for that noise level whose output (β_0) was the value at the top of the column.

this method. In the case of 1000 points and standard deviation of noise equal to 0.01, the ARE method in [13] returns the correct number of clusters for 62.67% of the trials, compared with the 100% in this method.

In Figures 1-8, we give several clustering results of the relative von Neumann entropy algorithm with different amounts of noise (as the ones in the table) and its respective entropy vs scale graph for a 500 sample points. The first of these is an example where the algorithm correctly classifies the clusters, and the second is where the algorithm fails. These were typical results for these trials, i.e. when the algorithm reported the correct number of clusters, the resulting clustering was also correct, and when it reported an incorrect number of clusters, the algorithm typically combined two or more clusters into one. We see from the figures that, even when our method reports an incorrect number of clusters, the reported clusters are well-separated from the others. The resulting classification will still likely be useful to an end user in such cases, and typically reflects the existence of a genuine gap between the clusters. Higher amounts of noise reduce the performance of the algorithm.

4.3. Comparison with other methods. We also compared our clustering algorithm with the *k-means* algorithm. For a 1000 points sample in the three interlinked circles we ran the three algorithms, in different amount of Gaussian noise. In addition to the sample of points, for the *k-means* algorithm we took as input the correct number of clusters $k = 3$. The results of these experiments are shown in the Figures 9-14. We see from the figures that the *k-means* algorithms incorrectly identified the clusters. Nonetheless, we consider this unsurprising, as these two algorithms are known to perform poorly on data in which the clusters have interesting geometry and which are not concentrated at a point.

4.4. Test on Image Data. In order to test our algorithm on image data, we used the unprocessed images from Columbia University Image Library (COIL-20) database. These images form a collection of 448×416-pixel gray scale images from 5 objects, each of which is photographed at 72 different rotation angles [12].

Regarding each image as a vector of pixel intensities in $\mathbb{R}^{448 \times 416}$ yields a set $X \subset \mathbb{R}^{448 \times 416}$ with 360 points; this set becomes a finite metric space when endowed with the ambient Euclidean distance. The result of applying our clustering algorithm to this set is the correct classification of all images in five clusters. We also calculated the results of applying the *k-means* and the *k*-NN algorithms to the same set. In the first case, we gave the data $k = 5$ as input and got an

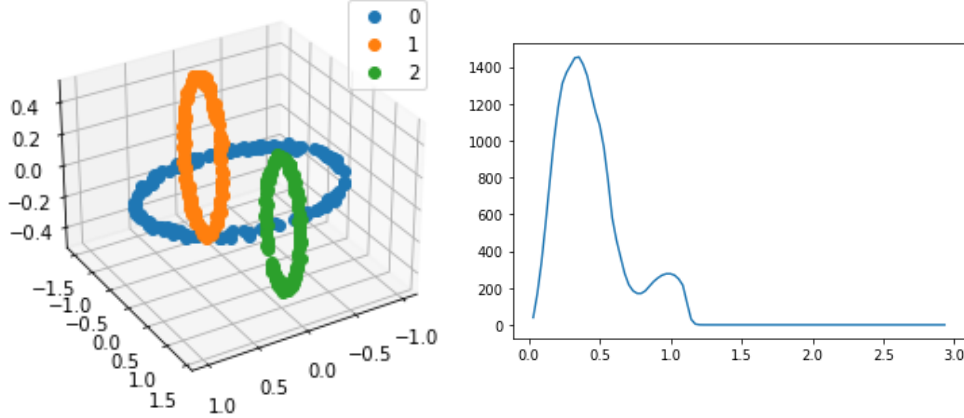


FIGURE 1. A typical example showing the correct classification of clusters. Noise $SD=0.01$. Left: Output of the algorithm. Right: Graph of relative von Neumann entropy (y-axis) vs. scale (x-axis).

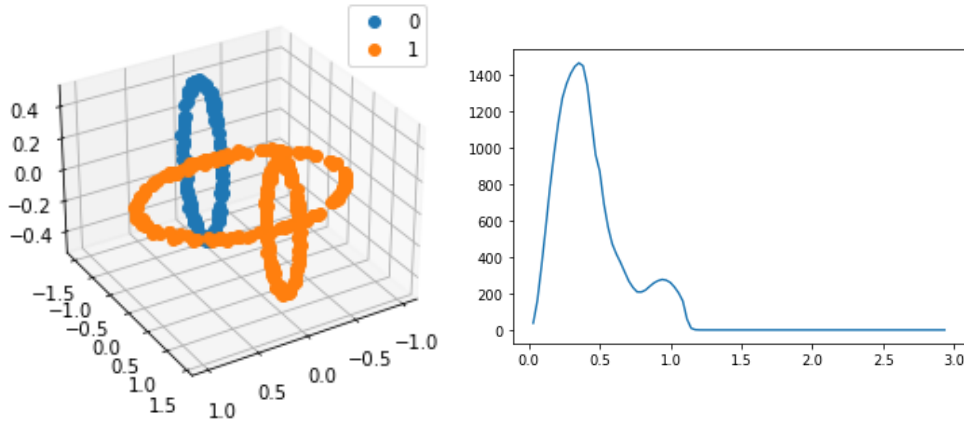


FIGURE 2. Incorrect classification of clusters. Noise $SD=0.01$. Left: Output of the algorithm. Right: Graph of Entropy (y-axis) vs. Scale (x-axis).

incorrect classification of 13 images. In the second case, we also took $k = 5$, obtaining an incorrect classification of 47 images. The results of each of these experiments are summarized in Figures 15-16.

4.5. Dimension Reduction. In order to test our dimension reduction algorithm, we tried the algorithm on several figures in three dimensions and reduced them to two dimensions. The results are found in Figures 17-20, where we see that the local geometry of the circular figures was largely preserved, and for the two-dimensional surfaces, points which were close in three-dimensions mostly stayed close in two-dimensions.

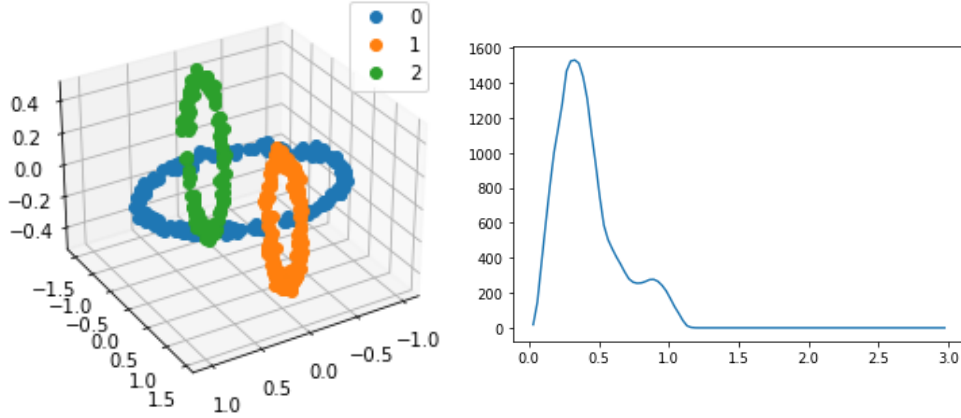


FIGURE 3. Correct classification of clusters. Noise SD=0.02. Left: Output of the algorithm. Right: Graph of Entropy (y-axis) vs. Scale.

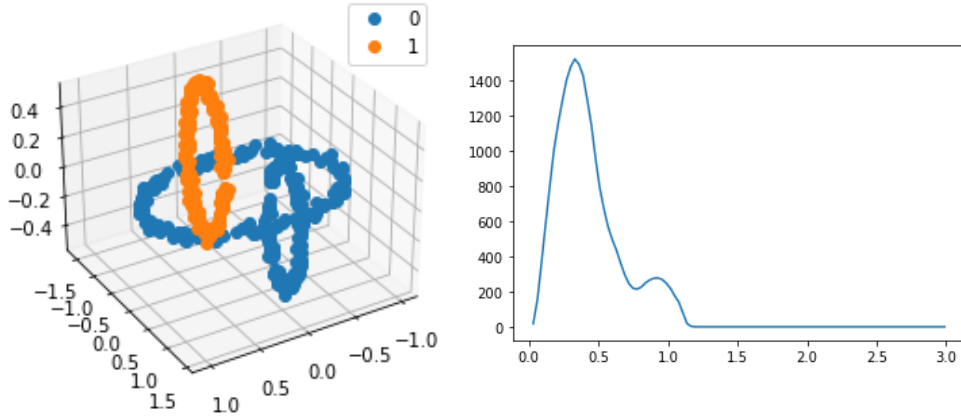


FIGURE 4. Incorrect classification of clusters. Noise SD=0.02. Left: Output of the algorithm. Right: Graph of Entropy (y-axis) vs. Scale (x-axis).

5. DISCUSSION AND FUTURE WORK

In this article, we have presented new clustering and dimension reduction algorithms for a data set S sampled from a uniform distribution on a metric measure space X , possibly corrupted by Gaussian noise, where X has been embedded in a larger metric space Z , and such that the metrics on X and Z are similar at small enough scales. The algorithms work by constructing a family of graphs indexed by the positive real numbers $r > 0$ which, roughly speaking, indicate the size of a local neighborhood around each point in the sample. We then identify an optimal scale $\hat{r} > 0$ by maximizing the relative von Neumann entropy of specially constructed heat operators based on the graphs. For clustering, we identify the clusters as the components of the associated graph

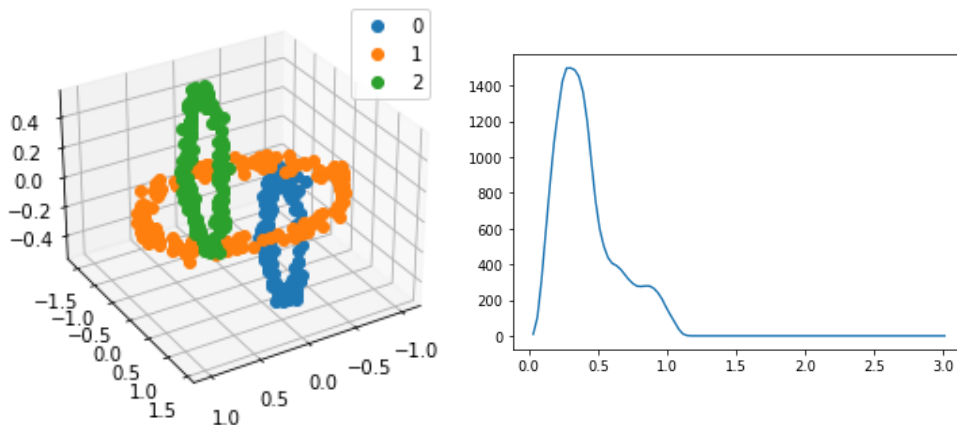


FIGURE 5. Correct classification of clusters. Noise SD=0.03. Left: Output of the algorithm. Right: Graph of Entropy (y-axis) vs. Scale (x-axis).

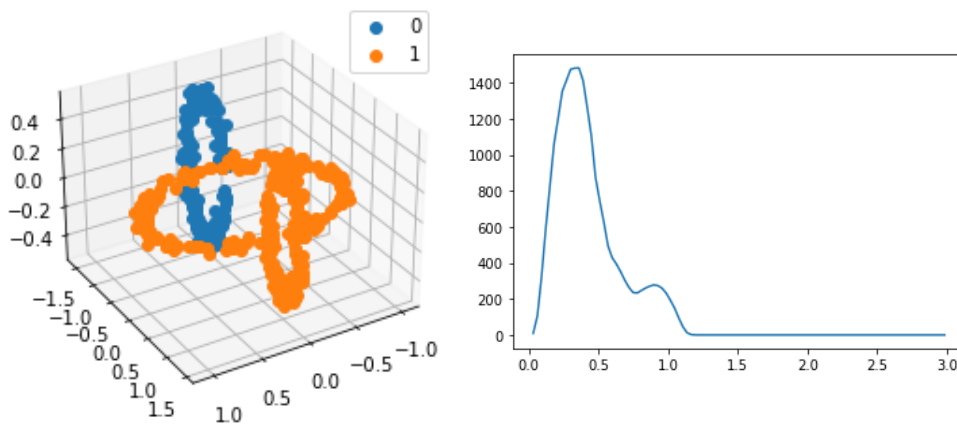


FIGURE 6. Incorrect classification of clusters. Noise SD=0.03. Left: Output of the algorithm. Right: Graph of Entropy (y-axis) vs. Scale (x-axis).

best approximate the same connected components as the space X , and for dimension reduction, we use the eigenvectors of the Laplacian $L_{\hat{r}}$ to construct a map $\Psi : S \rightarrow \mathbb{R}^k$. We have shown that the clustering algorithm represents a significant improvement over the Average Relative Entropy Method of [13], in addition to outperforming k -means clustering on the examples which we have shown here. A particularly interesting aspect of our construction is that the weights in our graphs are simply chosen to be the pairwise distance in the ambient space, in contrast to other spectral methods such as Laplacian Eigenmaps [3] and Diffusion Maps [7], where an ambient heat kernel is used.

There are a number of benefits to considering relative von Neumann entropy instead of an average of classical relative entropy as in [13], or even the semigroup-based heuristic of [15]. In

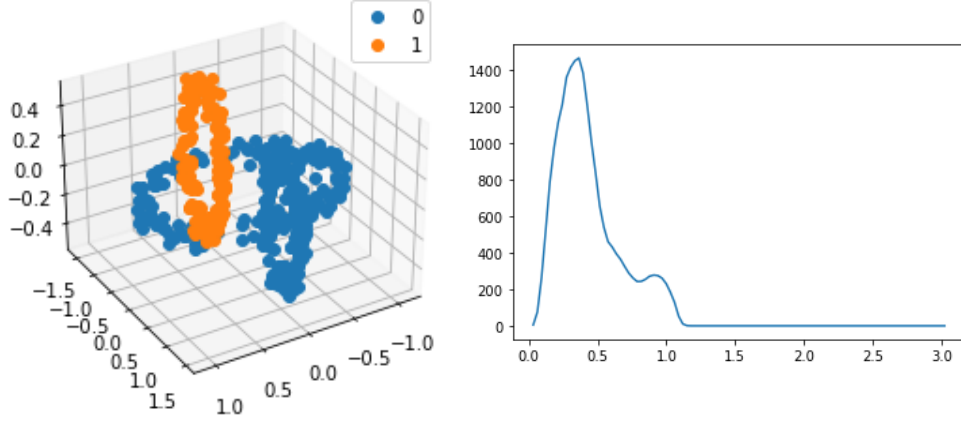


FIGURE 7. Incorrect classification of clusters. Noise SD=0.04. Left: Output of the algorithm. Right: Graph of Entropy (y-axis) vs. Scale (x-axis).

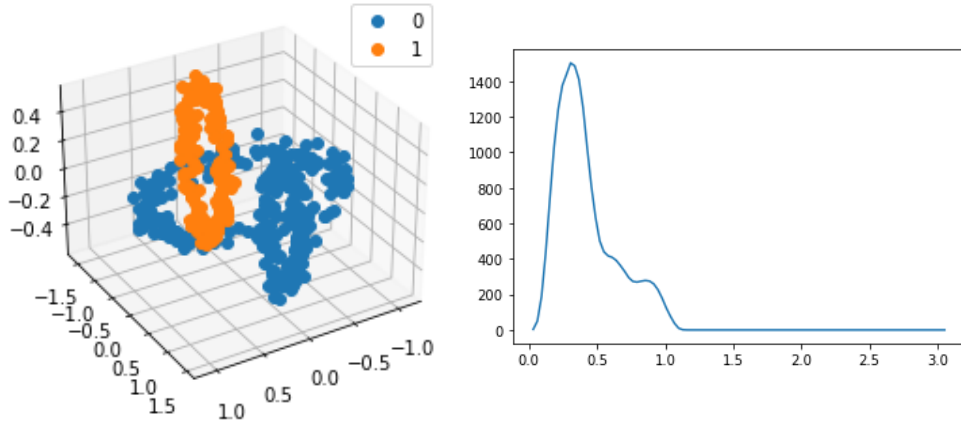


FIGURE 8. Incorrect classification of clusters. Noise SD=0.05. Left: Output of the algorithm. Right: Graph of Entropy (y-axis) vs. Scale (x-axis).

particular, von Neumann entropy is a natural noncommutative construction on the (normalized) heat operators, and we believe that this will make its rigorous theoretical treatment more tractable than the methods in either of [13] or [15], in addition to providing motivation and a setting for studying more noncommutative techniques in statistics.

We note three issues with this method which we hope to address in future work. First, the success of the clustering algorithm presented here depends strongly on the assumption that the sampling distribution is well-spread-out on its support - in this case, we used a uniform distribution - which unfortunately is not fulfilled in many interesting real-world examples. Extending this method to non-uniform distributions, in addition to dealing with a wider range of noise models, is an important avenue for future research. We also note that the method proposed here is, from a certain point of

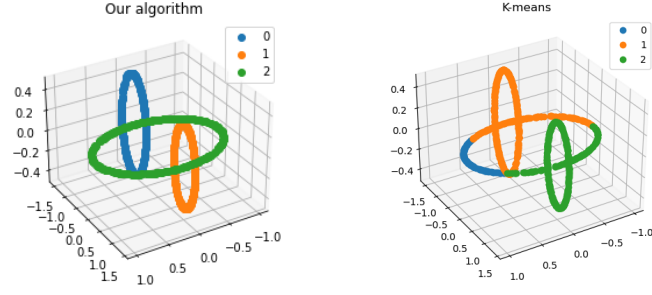


FIGURE 9. Comparison. No added noise. K-means: 244 mistakes

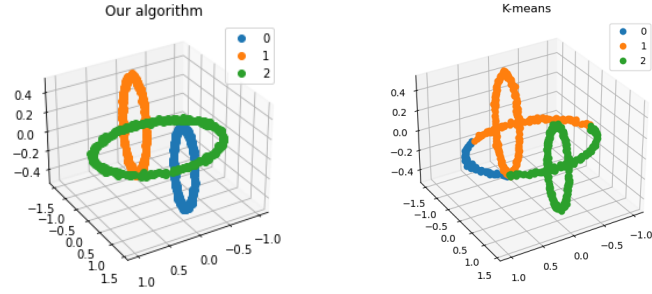


FIGURE 10. Comparison, SD=0.01. K-means: 233 mistakes

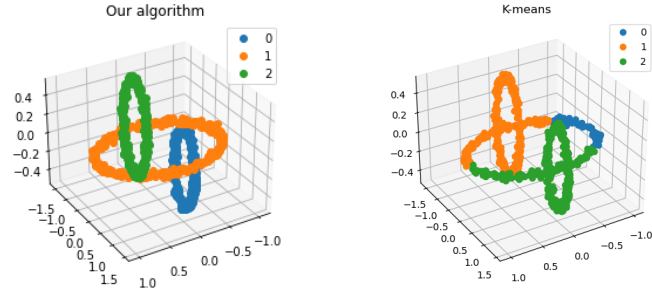
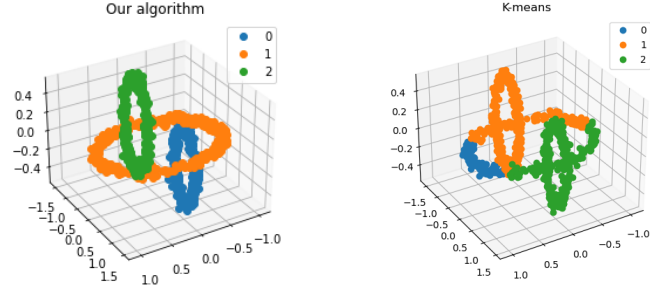
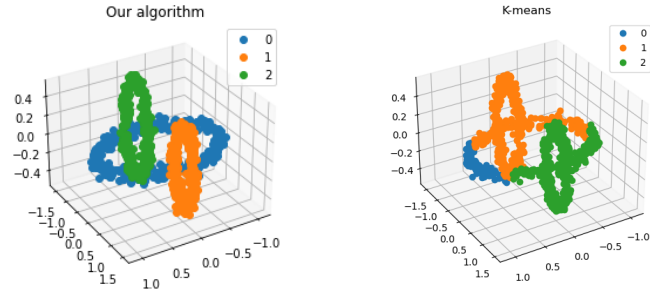
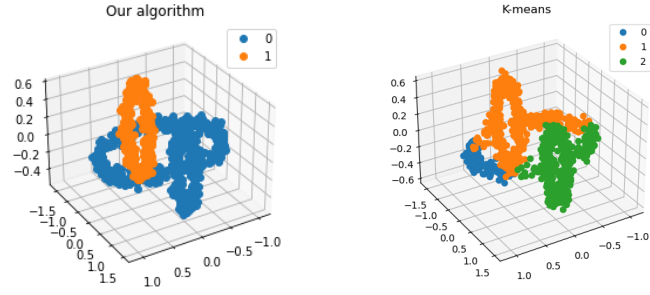


FIGURE 11. Comparison, SD=0.02. K-means: 255 mistakes

view, a refinement of single-linkage clustering (see [10], Section 4.2), and as such, it shares many of its shortcomings, in particular that it will produce ‘chaining’ artifacts that may occur in single-linkage clustering. Nonetheless, we also expect that the solutions which have been found for these issues in the case of single-linkage clustering will also work here with the appropriate modifications.

FIGURE 12. Comparison, $SD=0.03$. K-means: 237 mistakesFIGURE 13. Comparison, $SD=0.04$. K-means: 247 mistakesFIGURE 14. Comparison, $SD=0.05$. K-means: 248 mistakes

A further issue with the method which is currently unresolved is that computing the eigenvalues of large, dense matrices is computationally expensive. However, since the maxima of the relative von Neumann entropy appear to occur for relatively small values of the scale parameter $r > 0$, we are optimistic that future investigation will eliminate the need to consider matrices which are not sparse. Indeed, one may simply impose sparseness of the graphs as a constraint of the algorithm,

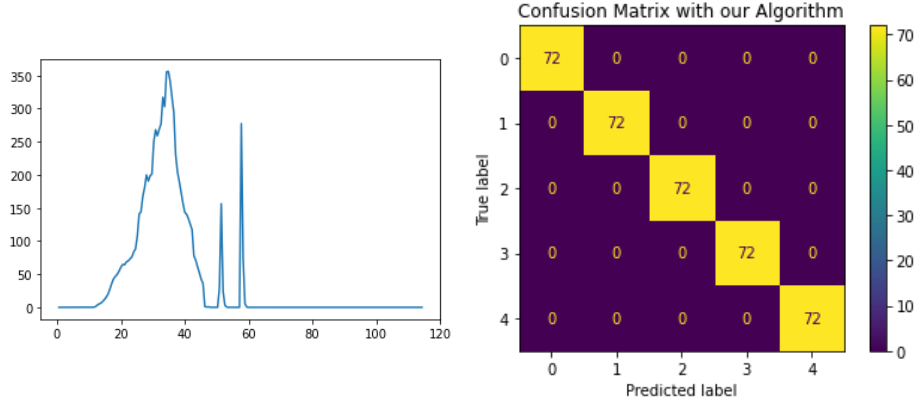


FIGURE 15. Performance of our algorithm for the COIL-20 unprocessed image data. Left: the Entropy graph, right: the Confusion Matrix.

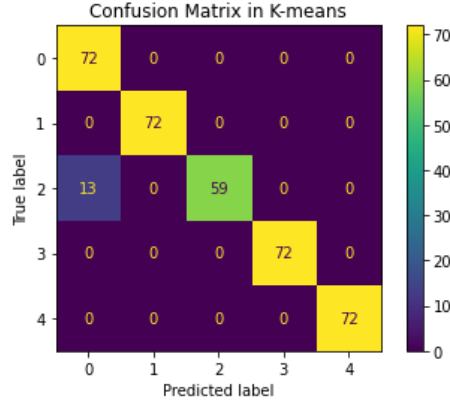


FIGURE 16. Confusion Matrix for the k -means algorithm applied to the COIL-20 unprocessed image data.

and then explore the effectiveness of this modification, but we believe that theoretical results that justify restricting consideration to sparse graphs may also be possible to find. Given the results we observed in our current experiments, however, we do not expect that restricting the algorithm to only consider sparse graphs would significantly affect the accuracy of the algorithms, but we do expect that it would significantly improve their speed.

Finally, the empirical success of the techniques introduced here introduces many interesting, difficult questions of how to establish performance guarantees for these methods.

CONFLICT OF INTEREST STATEMENT

The authors certify that they have no conflict of interest in the subject matter or materials discussed in this article.

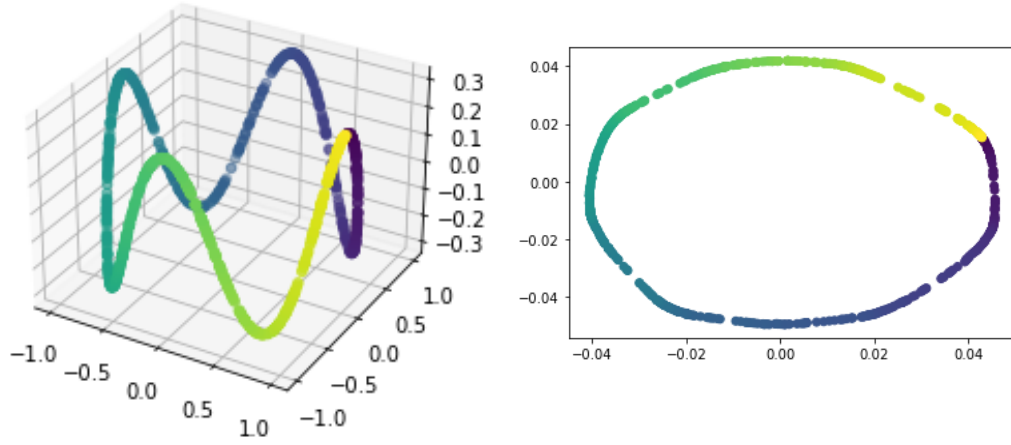


FIGURE 17. The corona and its two-dimensional reduction.

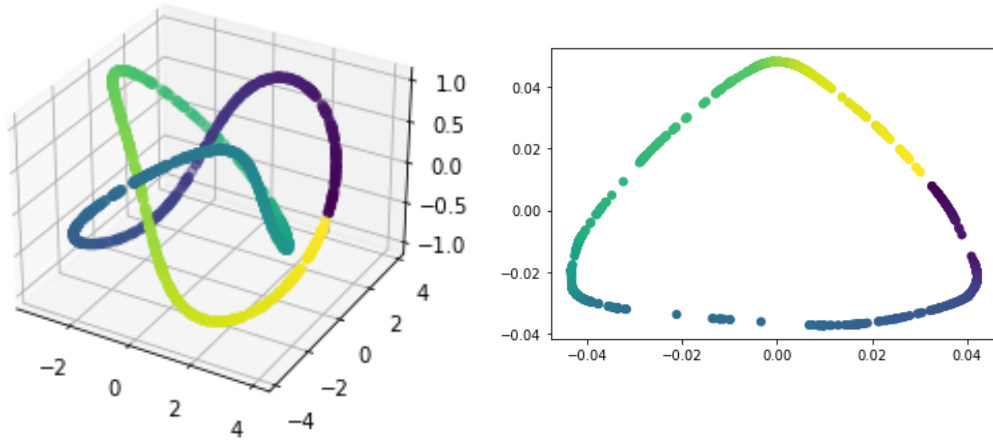


FIGURE 18. A trefoil knot and its two-dimensional reduction

REFERENCES

- [1] Muhammad Sirajo Abdullahi, Poom Kumam, and P. Christopher Staecker. "Digital Lefschetz numbers and related fixed point theorems". In: *Rev. R. Acad. Cienc. Exactas Fís. Nat. Ser. A Mat. RACSAM* 116.4 (2022), Paper No. 173, 23. ISSN: 1578-7303,1579-1505. DOI: 10.1007/s13398-022-01318-1. URL: <https://doi-org.biblio.cimat.remotexs.co/10.1007/s13398-022-01318-1>.
- [2] Ralph Abraham and Joel Robbin. *Transversal Mappings and Flows*. W.A. Benjamin, Inc., 1967.

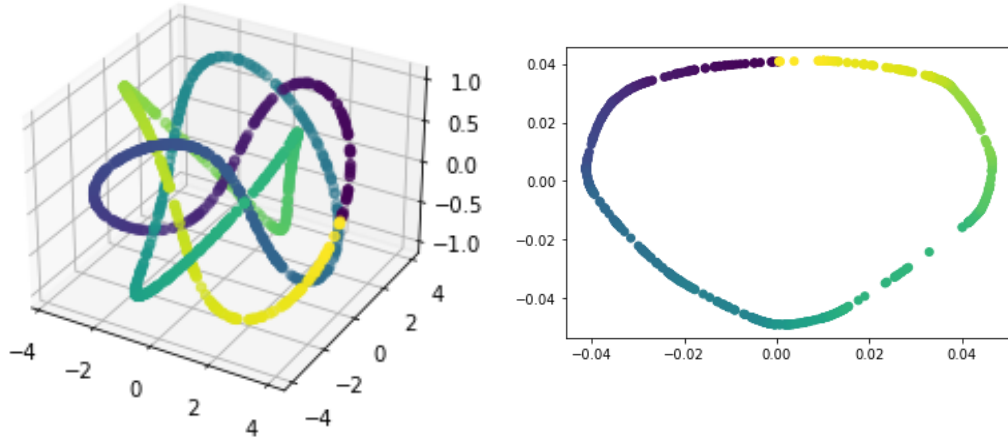


FIGURE 19. A torus knot and its two-dimensional reduction

Swiss Roll in Ambient Space

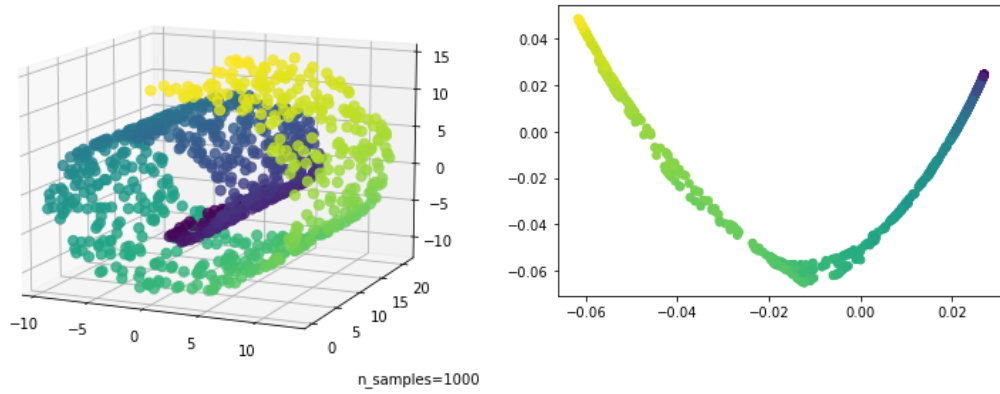


FIGURE 20. The Swiss roll.

- [3] Mikhail Belkin and Partha Niyogi. “Laplacian Eigenmaps for Dimensionality Reduction and Data Representation”. In: *Neural Comput.* 15.6 (June 2003), pp. 1373–1396. ISSN: 0899-7667. DOI: 10.1162/089976603321780317. URL: <http://dx.doi.org/10.1162/089976603321780317>.
- [4] P. Bérard, G. Besson, and S. Gallot. “Embedding Riemannian manifolds by their heat kernel”. In: *Geom. Funct. Anal.* 4.4 (1994), pp. 373–398. ISSN: 1016-443X. DOI: 10.1007/BF01896401. URL: <https://doi.org/10.1007/BF01896401>.

- [5] Frédéric Chazal et al. “Persistence-Based Clustering in Riemannian Manifolds”. In: *J. ACM* 60.6 (Nov. 2013). ISSN: 0004-5411. DOI: 10.1145/2535927. URL: <https://doi.org/10.1145/2535927>.
- [6] Fan R. K. Chung. *Spectral graph theory*. Vol. 92. CBMS Regional Conference Series in Mathematics. Published for the Conference Board of the Mathematical Sciences, Washington, DC; by the American Mathematical Society, Providence, RI, 1997, pp. xii+207. ISBN: 0-8218-0315-8.
- [7] Ronald R. Coifman and Stéphane Lafon. “Diffusion maps”. In: *Appl. Comput. Harmon. Anal.* 21.1 (2006), pp. 5–30. ISSN: 1063-5203. DOI: 10.1016/j.acha.2006.04.006. URL: <http://dx.doi.org/10.1016/j.acha.2006.04.006>.
- [8] John B. Conway. *A course in functional analysis*. Second. Vol. 96. Graduate Texts in Mathematics. Springer-Verlag, New York, 1990, pp. xvi+399. ISBN: 0-387-97245-5.
- [9] David L. Donoho and Carrie Grimes. “Hessian eigenmaps: locally linear embedding techniques for high-dimensional data”. In: *Proc. Natl. Acad. Sci. USA* 100.10 (2003), pp. 5591–5596. ISSN: 0027-8424,1091-6490. DOI: 10.1073/pnas.1031596100. URL: <https://doi.org/10.1073/pnas.1031596100>.
- [10] Brian S. Everitt et al. *Cluster analysis*. Fifth. Wiley Series in Probability and Statistics. John Wiley & Sons, Ltd., Chichester, 2011, pp. xvi+330. ISBN: 978-0-470-74991-3. DOI: 10.1002/9780470977811. URL: <https://doi.org/10.1002/9780470977811>.
- [11] Trevor Hastie, Robert Tibshirani, and Jerome Friedman. *The Elements of Statistical Learning*. Second. Springer Series in Statistics. Data mining, inference, and prediction. Springer, New York, 2009, pp. xxii+745. ISBN: 978-0-387-84857-0. DOI: 10.1007/978-0-387-84858-7. URL: <https://doi.org/10.1007/978-0-387-84858-7>.
- [12] S.A. Nene, S.K. Nayar, and H. Murase. *Columbia Object Image Library (COIL-20)*,”. Tech. rep. Columbia University, 1996.
- [13] Antonio Rieser. “A topological approach to spectral clustering”. In: *Foundations of Data Science* 3.1 (2021), pp. 49–66.
- [14] Sam T. Roweis and Lawrence K. Saul. “Nonlinear Dimensionality Reduction by Locally Linear Embedding”. In: *Science* 290.5500 (2000), pp. 2323–2326. DOI: 10.1126/science.290.5500.2323. eprint: <https://www.science.org/doi/pdf/10.1126/science.290.5500.2323>. URL: <https://www.science.org/doi/abs/10.1126/science.290.5500.2323>.
- [15] Shan Shan and Ingrid Daubechies. *Diffusion Maps : Using the Semigroup Property for Parameter Tuning*. 2022. arXiv: 2203.02867 [stat.ML]. URL: <https://arxiv.org/abs/2203.02867>.
- [16] Wen-Jun Shen et al. “Introduction to the Peptide Binding Problem of Computational Immunology: New Results”. English. In: *Foundations of Computational Mathematics* 14.5 (2014), pp. 951–984. ISSN: 1615-3375. DOI: 10.1007/s10208-013-9173-9. URL: <http://dx.doi.org/10.1007/s10208-013-9173-9>.
- [17] A. Singer and H.-T. Wu. “Vector diffusion maps and the connection Laplacian”. In: *Comm. Pure Appl. Math.* 65.8 (2012), pp. 1067–1144. ISSN: 0010-3640. DOI: 10.1002/cpa.21395. URL: <http://dx.doi.org/10.1002/cpa.21395>.
- [18] Joshua B. Tenenbaum, Vin de Silva, and John C. Langford. “A Global Geometric Framework for Nonlinear Dimensionality Reduction”. In: *Science* 290.5500 (2000), pp. 2319–2323. DOI: 10.1126/science.290.5500.2319. eprint: <https://www.science.org/doi/pdf/10.1126/science.290.5500.2319>. URL: <https://www.science.org/doi/abs/10.1126/science.290.5500.2319>.

- [19] Mark M. Wilde. *Quantum information theory*. Second. Cambridge University Press, Cambridge, 2017, pp. xvii+757. ISBN: 978-1-107-17616-4. DOI: 10.1017/9781316809976. URL: <https://doi.org/10.1017/9781316809976>.
- [20] Zhen-yue Zhang and Hong-yuan Zha. “Principal manifolds and nonlinear dimensionality reduction via tangent space alignment”. In: *Journal of Shanghai University (English Edition)* 8.4 (2004), pp. 406–424. DOI: 10.1007/s11741-004-0051-1. URL: <https://doi.org/10.1007/s11741-004-0051-1>.

CENTRO DE INVESTIGACIÓN EN MATEMÁTICAS, A.C., CALLE JALISCO S/N, COLONIA VALENCIANA, GUANAJUATO
C.P. 36023, GUANAJUATO, MÉXICO

Email address: `araceli.guzman@cimat.mx,antonio.rieser@cimat.mx`